Short communication

Reconstruction of white matter fibre tracts using diffusion kurtosis tensor imaging at 1.5T: Pre-surgical planning in patients with gliomas

Joao Leote[a,b,*], Rita G. Nunes[c], Luis Cerqueira[d], Ricardo Loução[a], Hugo A. Ferreira[a]

[a] Instituto de Biofísica e Engenharia Biomédica, Faculdade de Ciências da Universidade de Lisboa, Lisbon, Portugal
[b] Neurosurgery Department, Hospital Garcia de Orta, Almada, Portugal
[c] Institute for Systems and Robotics (LARSyS) and Department of Bioengineering, Instituto Superior Técnico, University of Lisbon, Lisbon, Portugal
[d] Neuroradiology Department, Centro Hospitalar Lisboa Central, Lisbon, Portugal

ARTICLE INFO

ABSTRACT

Tractography studies for pre-surgical planning of primary brain tumors is typically done using diffusion tensor imaging (DTI), which cannot resolve crossing, kissing or highly angulated fibres. Tractography based on the estimation of the diffusion kurtosis (DK) tensor was recently demonstrated to enable tackling these limitations. However, its use in the clinical context at low 1.5T field has not yet been reported.

Purpose: To evaluate if the estimation of whole-brain tractography using the DK tensor is feasible for pre-surgical investigation of patients with brain tumors at 1.5T.

Methods: Eight healthy subjects and 3 patients with brain tumors were scanned at 1.5T using a 12-channel head coil. Diffusion-weighted images were acquired with repetition/echo times of 5800/107 ms, 82×82 resolution, $3 \times 3 \times 3\,\mathrm{mm}^3$ voxel size, b-values of 0, 1000, 2000 s/mm^2 and 64 gradient sensitising directions. Whole-brain tractography was estimated using the DK tensor and corticospinal tracts (CST) were isolated using regions-of-interest placed at the cerebral peduncles and motor gyrus. Tract size, DK metrics and CST deviation index (highest curvature point) were compared between healthy subjects and patients.

Results: Tract sizes did not differ between groups. The CST deviation index was significantly higher in patients compared to healthy subjects. Fractional anisotropy was significantly lower in patients, with higher mean kurtosis asymmetry index at the highest curvature point in patients.

Conclusions: Corticospinal fibre bundles estimated using DK tensor in a 1.5T scanner presented similar properties in patients with brain gliomas as those reported in the literature using DTI-based tractography.

1. Introduction

The first magnetic resonance (MR) scanners used for advanced imaging had a field of 1.5T and are still widely employed nowadays [1]. Among such applications are diffusion tensor (DTI) and kurtosis imaging (DKI), used for studying tissue microstructure [2]. A recent report found that 3T systems provide a minor advantage in the estimation of kurtosis measures when compared to 1.5T systems [3]. However, no study has yet assessed the feasibility of reconstructing white matter fibres using DKI at 1.5T.

In this study we tested whether DKI can provide clinically acceptable whole-brain tractography reconstructions at 1.5T in both healthy volunteers and brain tumor patients. In particular we looked for high curvatures in the corticospinal tracts (CST).

2. Methods

2.1. Subjects and patients

Eight healthy volunteers (two males, mean age 22, ranging from 20 to 26 years old) and three patients (2 males, mean age 27, ranging from 24 to 30) diagnosed with brain astrocytoma were recruited for an MRI scan (Fig. 1). The study was approved by the hospital's ethics committee and prior informed written consent was obtained from each individual.

2.2. Magnetic resonance imaging protocol

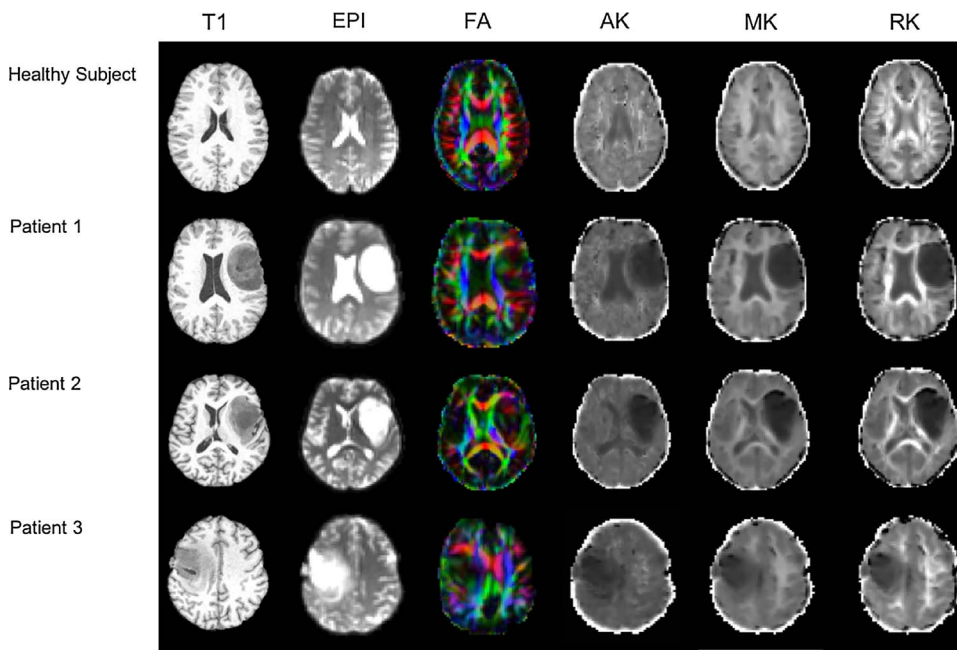A 1.5T Avanto (Siemens, Erlangen, Germany) MRI scanner with a

Fig. 1. Transverse contrast-enhanced T1-weighted images (T1), echo planar images (EPI), fractional anisotropy (FA) maps and diffusion kurtosis invariant metrics (AK: axial kurtosis; MK: mean kurtosis; RK: radial kurtosis) maps of a healthy subject and patients with gliomas. Note the distortion of the fibres with cranial-caudal direction (i.e. coloured in blue) produced by the tumor in the pathological hemispheres. (For interpretation of the references to colour in this figure legend, the reader is referred to the web version of this article.)

12-channel head receiver coil was used. The scanning protocol included a volumetric $1 \times 1 \times 1 \, mm^3$ T1-weighted followed by a DWI sequence. Additionally, patients were injected with gadolinium contrast agent and a second T1-weighted image was acquired. DWI were acquired along 64 non-collinear gradient sensitising directions using b-values of 0, 1000, and 2000 s/mm^2 with a single-shot spin-echo imaging sequence with the following parameters: repetition time = 5800 ms, echo time = 107 ms, 82×82 acquisition matrix resolution; field-of-view of $230 \times 230 \, mm^2$, 42 slices without gaps, with a $3 \times 3 \times 3 \, mm^3$ voxel size.

2.3. DWI pre-processing and DKI processing

All images were corrected for motion and eddy current geometric distortions and non-brain tissues were removed using, respectively, the *eddy* tool [4] and the Brain Extraction Tool [5] from FMRI Software Library (FSL; http://fsl.fmrib. ox.ac.uk/fsl).

To estimate DTI and DK tensor metrics, the toolbox United-DKI was used [6], which includes DK tractography reconstruction based on kurtosis maxima, as described by Neto-Henriques and colleagues [7].

Tracking was performed in regions with Fractional Anisotropy (FA) greater than 0.2 and with a maximum curvature of 35° between principal eigenvectors in adjacent voxels. The tractography results were visualized using Trackvis (http://www.trackvis.org/).

2.4. Data reduction and statistical analysis

Whole-brain tractography was performed and its metrics computed (streamline count, voxel count) in all subjects using Trackvis. We isolated the CST by seeding from the cerebral peduncles and the motor pre-central gyrus, using anatomical images and FA maps to evaluate its course in all subjects. We also extracted CST size for comparison between pathological and healthy hemispheres.

In order to observe the mass effect produced in the reconstructed fibre bundles by the tumor, we calculated the distances between the CST fibre tracts and the brain midline along the z-axis, using FSLView (FSL; http://fsl.fmrib. ox.ac.uk/fsl). From these, the highest distance was extracted, for both the pathologic (p) and healthy (h) hemispheres, and the deviation index (DI) was calculated, as defined by:

$$DI = \left| \frac{(Deviation \;\; Distance \;\; h) - (Deviation \;\; Distance \;\; p)}{(Deviation \;\; Distance \;\; h) + (Deviation \;\; Distance \;\; p)} \right| \quad (1)$$

We then placed a region-of-interest at the voxels (i.e. $3 \times 3 \times 3$ size) with highest curvature point of the CST and obtained both DTI (FA; mean, axial and radial diffusivities) and DKI (mean, axial and radial kurtosis) invariant metrics, to calculate the asymmetry index between hemispheres for each metric as performed for the DI.

Using SPSS (IBM Inc., Chicago, USA), the Mann-Whitney U test was used to compare reconstructed tract sizes and estimated DTI/DKI metrics between healthy subjects and patients, at a significance level of 95%.

3. Results

3.1. MRI processing protocol and tractography

Fig. 1 shows representative examples of structural T1, echo planar images, FA and DK invariant metrics images of a healthy subject and of all patients. Whole-brain tractography and isolated CST size for a healthy subject and patients can be found in Fig. 2. No significant differences in size were found between healthy and patient groups, in either whole-brain or CST, despite a tendency being observed for the number of depicted voxels (Fig. 2B; p = 0.069). In Fig. 2C are showed the delineated CST of a healthy subject and patients.

3.2. Analysis of the highest deviation region

The DTI and DKI metrics extracted from the highest curvature point of the CST are summarized in Table 1. The DI was significantly larger in pathological hemispheres (p = 0.0013). Mean FA values and their asymmetry indices were significantly higher (p = 0.01), as well as radial diffusivity (p = 0.026) in healthy subjects when compared to patients. None of the DKI metrics showed significant changes in the group comparison, except for the mean kurtosis asymmetry index which was higher in patients (p = 0.04).
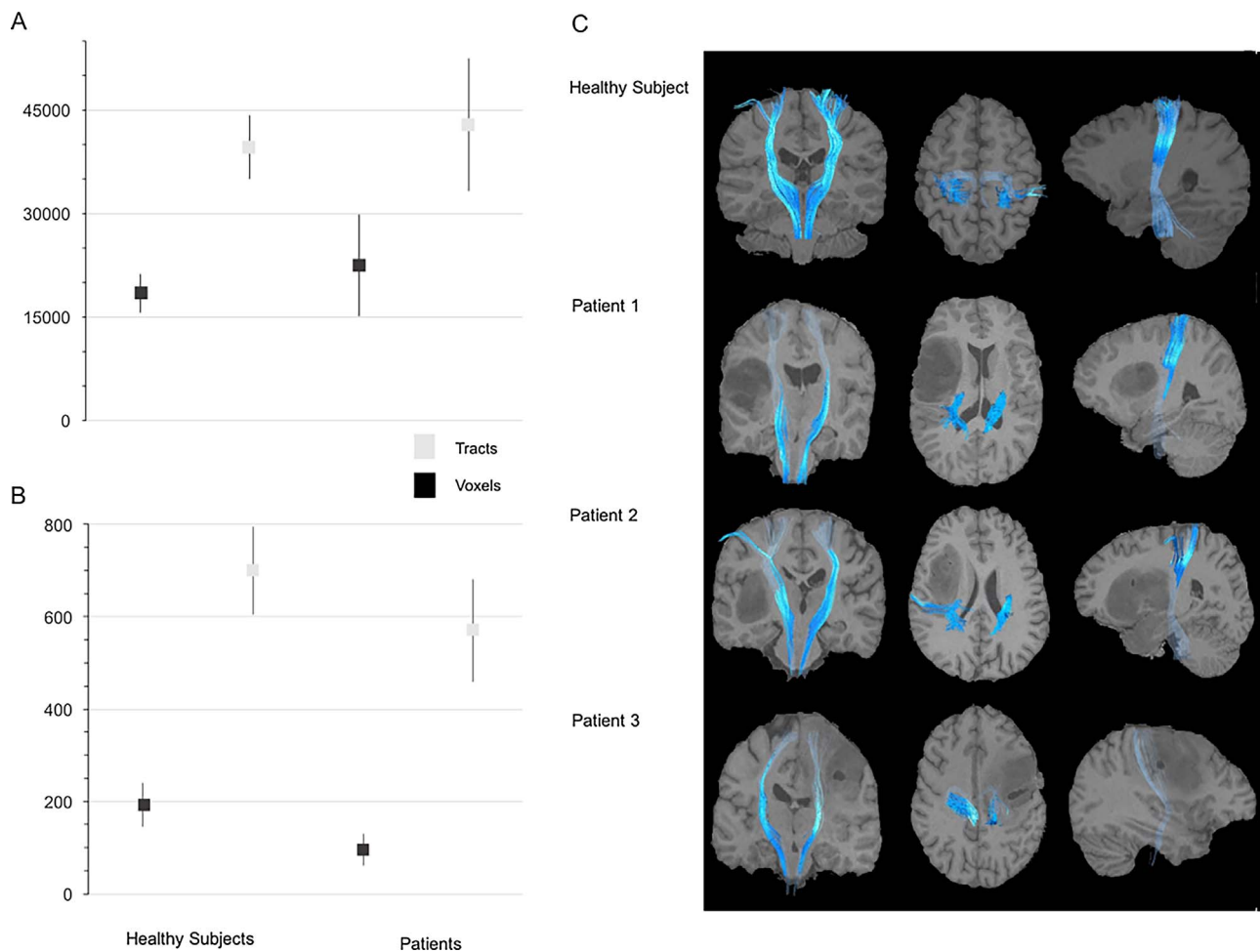
Fig. 2. Mean tract sizes for whole-brain (A) and corticospinal (B) tractography of healthy subjects and patients groups (error bars translate standard deviation). Statistically significant differences in tracts and voxel numbers between groups were not found despite the smaller standard deviation in patients' corticospinal tract (CST) size. Representative streamlined fibre bundles of CST are also presented (C). Note the pronounced mass effect imposed by the tumor presence in CST's and their close proximity.

4. Discussion

4.1. DWI acquisition and tractography

The ability to streamline white matter fibre bundles in healthy subjects using DKI has already been reported, [7–10] showing improvements from DTI. However, previous studies were conducted using 3T scanners.

We acquired DKI using a 1.5T scanner, and assessed whether tractography reconstruction is affected by the inherently lower signal-to-noise ratio. The protocol used in both healthy and tumor patients is compatible with most clinical departments [11].

Although many studies point towards the use of several b-values for the DK tensor estimation [7,8], clinically compatible DKI sequences with just 3 b-values have also been suggested. However, none was studied in a 1.5T system. Marrale and colleagues (2015) [2] suggested the use of 32 directions to estimate DKI metrics at shorter scan times. Our protocol used 64 directions, as the higher number of directions increases spatial-dependency discrimination of the diffusion profile, relevant for a better characterization of complex tissues. Additionally, it can help mitigate the effects of the lower 1.5T signal-to-noise ratio.

4.2. Effect of brain neoplasm in DK-based tractography

In order to assess if the distortion produced by the tumor affected the number of reconstructed tracts, we compared the size of whole-brain tracts and CST of patients to those of healthy volunteers. We

found no statistical differences between the groups. However, due to the small sample size, these results cannot be generalised. In fact, the number of depicted voxels in CST showed a tendency to be diminished in patients (Fig. 2B).

The presence of a brain tumor causes histological distortion and consequently increases the brain microstructure complexity [12]. Thus, the CST is most likely to be stressed by mass effect at its highest deviation region.[13] Therefore, we analysed the highest curvature point of CST as a higher tissue complexity could affect the DTI/DKI metrics performance and consequently their ability to reconstruct fibres.

We found a significantly increased DI in patients due to mass effects similar to previous DTI tractography studies [14] and significantly decreased mean kurtosis in patients, compatible with an increased Gaussian diffusion behaviour which was not observed in healthy subjects (Table 1). This hypothesis is supported by the presence of tumor surrounding edema lowering mean FA values. [15] We also found increased radial diffusivity in patients, which was expected due to the presence of low grade gliomas with minor neurological involvement and preserved white matter, despite the possibility of some myelin degradation [14].

We show that at the highest deviation region the DTI metrics are more affected than DKI metrics, as supported by the higher proportional decrease of mean FA values in comparison with mean kurtosis values in patients (decrease of 0.31 vs 0.19, respectively; Table 1). This leads us to believe that in the deviation region, DTI's ability to accurately reconstruct fibre tracts is limited. In turn, DKI-based tractography is resilient to this phenomenon, due to DKI's ability to better

Table 1
Diffusion metrics, asymmetry index and deviation of delineated corticospinal tracts.

Patients	FA	MD[b]	AD[b]	RD[b]	MK[b]	AK[b]	RK[b]	DI
1	0.2 (0.4)[a]	0.9 (0.1)	2.3 (0.1)	1.3 (0.1)	1.0 (0.04)	0.7 (0.02)	1.1 (0.1)	0.17
2	0.3 (0.2)	1.1 (0.1)	1.7 (0.2)	1.4 (0.1)	1.0 (0.03)	0.6 (0.01)	1.2 (0.2)	0.12
3	0.2 (0.4)	0.9 (0.2)	1.6 (0.2)	1.4 (0.2)	0.8 (0.04)	0.5 (0.01)	1.0 (0.1)	0.14
Mean ± SD	0.23* ± 0.06 (0.24)*	0.96 ± 0.11 (0.009)	1.8 ± 0.10 (0.008)	1.3* ± 0.15 (0.18)*	0.89 ± 0.11 (0.14)*	0.60 ± 0.05 (0.09)	1.14 ± 0.11 (0.07)	0.14* ± 0.03
Healthy subjects group Mean ± SD	0.54 ± 0.03 (0.04)	0.86 ± 0.06 (0.002)	1.7 ± 0.10 (0.006)	0.8 ± 0.09 (0.05)	1.08 ± 0.10 (0.02)	0.84 ± 0.12 (0.03)	1.28 ± 0.32 (0.03)	0.02 ± 0.03

FA – Fractional anisotropy; MD – Mean diffusivity; AD – Axial diffusivity; RD – Radial diffusivity; MK – Mean kurtosis; AK – Axial kurtosis; RK – Radial kurtosis; DI – Deviation index of corticospinal tract; SD – standard deviation.
[a] The values between parenthesis refer to the asymmetry index in comparison with the contralateral hemisphere.
[b] Diffusivities are presented in units of 10^{-3} mm^2/s.
* Statistically significant ($p < 0.05$) differences for evaluated parameter values between healthy subjects and patients.

characterize complex microstructures [7,8,12].

For pre-surgical planning, distance between the tumor and tracts is of most interest, in order to avoid neurological morbidities. However, this observation remains to be further analysed and tested using direct electrical stimulation, comparing the distance between the point of stimulus and the tracts delineated by DTI and DK-based tractography.

In conclusion, the present study reports the feasibility of the DK-based tractography method in patients with brain gliomas, reconstructed from DWI acquired at 1.5T with a readily-available MRI acquisition protocol.

Conflicts of interest

The authors have nothing to declare.

Funding sources

Acknowledgements

References

[1] L. Martí-Bonmatí, M. Kormano, MR equipment acquisition strategies: low-field or high-field scanners, Eur. Radiol. 7 (Suppl. 5) (1997) 263–268.
[2] M. Marrale, G. Collura, M. Brai, N. Toschi, F. Midiri, G. La Tona, A. Lo Casto, C. Gagliardo, Physics, techniques and review of neuroradiological applications of Diffusion Kurtosis Imaging (DKI), Clin. Neuroradiol. 20 (2015) 1–13.
[3] C.B. Shaw, J.H. Jensen, R.L. Deardorff, M.V. Spampinato, J.A. Helpern, Comparison of diffusion metrics obtained at 1.5T and 3T in human brain with diffusional kurtosis imaging, J. Magn. Reson. Imaging 45 (2017) 673–680.
[4] J.L.R. Andersson, S.N. Sotiropoulos, An integrated approach to correction for off-resonance effects and subject movement in diffusion MR imaging, Neuroimage 15 (125) (2016) 1063–1078.
[5] S.M. Smith, Fast robust automated brain extraction, Hum. Brain Mapp. 17 (2002) 143–155.
[6] R. Neto-Henriques, H.A. Ferreira, M.M. Correia, United Diffusion Kurtosis Imaging (UDKI) toolbox, MAGMA 28 (2015) 511–512.
[7] R. Neto-Henriques, M.M. Correia, R.G. Nunes, H.A. Ferreira, Exploring the 3D geometry of the diffusion kurtosis tensor–impact on the development of robust tractography procedures and novel biomarkers, Neuroimage 111 (2015) 85–99.
[8] M. Lazar, J.H. Jensen, L. Xuan, J.A. Helpern, Estimation of the orientation distribution function from diffusional kurtosis imaging, Magn. Reson. Med. 60 (2008) 774–781.
[9] G.R. Glenn, J.A. Helpern, A. Tabesh, J.H. Jensen, Optimization of white matter fiber tractography with diffusional kurtosis imaging, NMR Biomed. 28 (2015) 1245–1256.
[10] G.R. Glenn, L.W. Kuo, Y.P. Chao, C.Y. Lee, J.A. Helpern, J.H. Jensen, Mapping the orientation of white matter fiber bundles: a comparative study of diffusion tensor imaging, diffusional kurtosis imaging, and diffusion spectrum imaging, AJNR Am. J. Neuroradiol. 37 (2016) 1216–1222.
[11] B.M. Ellingson, M. Bendszus, J. Boxerman, D. Barboriak, B.J. Erickson, M. Smits, S.J. Nelson, E. Gerstner, B. Alexander, G. Goldmacher, W. Wick, M. Vogelbaum, M. Weller, E. Galanis, J. Kalpathy-Cramer, L. Shankar, P. Jacobs, W.B. Pope, D. Yang, C. Chung, M.V. Knopp, S. Cha, M.J. van den Bent, S. Chang, W.K. Yung, T.F. Cloughesy, P.Y. Wen, M.R. Gilbert, Jumpstarting brain tumor drug development coalition imaging standardization steering committee. Consensus recommendations for a standardized brain tumor imaging protocol in clinical trials, Neuro Oncol. 17 (2015) 1188–1198 (Review).
[12] J. Jensen, J. Helpern, MRI quantification of non-Gaussian water diffusion by kurtosis analysis, NMR Biomed. 23 (2010) 698–710.
[13] A.R. Potgieser, M. Wagemakers, A.L. van Hulzen, B.M. de Jong, E.W. Hoving, R.J. Groen, The role of diffusion tensor imaging in brain tumor surgery: a review of the literature, Clin. Neurol. Neurosurg. 124 (2014) 51–58.
[14] T. Nguyen-Thanh, M. Reisert, C. Anastasopoulos, F. Hamzei, T. Reithmeier, M.S. Vry, V.G. Kiselev, A. Weyerbrock, I. Mader, Global tracking in human gliomas: a comparison with established tracking methods, Clin. Neuroradiol. 23 (2013) 263–275.
[15] S. Van Cauter, J. Veraart, J. Sijbers, R.R. Peeters, U. Himmelreich, F. De Keyzer, S.W. Van Gool, F. Van Calenbergh, S. De Vleeschouwer, W. Van Hecke, S. Sunaert, Gliomas: diffusion kurtosis MR imaging in grading, Radiology 263 (2012) 492–501.